

P. PAL-VAL\*<sup>#</sup>, L. PAL-VAL\*, V. NATSIK\*, A. DAVYDENKO\*\*, A. RYBALKO\*\*\*

## GIANT YOUNG'S MODULUS VARIATIONS IN ULTRAFINE-GRAINED COPPER CAUSED BY TEXTURE CHANGES AT POST-SPD HEAT TREATMENT

### GIGANTYCZNE ZMIANY MODUŁU YOUNGA W ULTRA DROBNOZIARNISTEJ MIEDZI SPOWODOWANE PRZEZ ZMIANY TEKSTURY W TRAKCIE OBRÓBKIE CIEPLNEJ PO SPD

The effect of annealing on dynamic Young's modulus,  $E$ , of ultrafine-grained (UFG) copper obtained by combined severe plastic deformation (SPD) is investigated. It is established that Young's modulus in the SPD-prepared samples exceeds that in the coarse-grained fully annealed (CGFA) samples by 10 to 20 %. Isothermal annealing at elevated temperatures between 90 and 630°C leads to a sharp decrease of Young's modulus for annealing temperatures above 210°C. After annealing at 410°C, the value of  $E$  reaches its minimal value that is 35 % lower than  $E$  in CGFA samples (total change in  $E$  is about 47 % of the initial value). Further annealing at higher temperatures leads to an increase in Young's modulus. It is shown, that the unusual behavior of Young's modulus is caused by formation of the  $\langle 111 \rangle$  axial texture in the SPD-treated samples which then is replaced by the  $\langle 001 \rangle$  texture during the post-SPD heat treatment.

*Keywords:* elastic properties, Young's modulus, severe plastic deformation, crystallographic texture

Zbadano wpływ wyżarzania na dynamiczny moduł Younga ( $E$ ), w ultra drobnoziarnistej miedzi (UFG) otrzymanej przez złożone intensywne odkształcenie plastyczne (SPD). Stwierdzono, że wartość modułu Younga próbek przygotowanych przez SPD przekracza tą w gruboziarnistych w pełni wyżarzonych próbkach (CGFA) o 10 do 20%. Izotermiczne wyżarzanie w podwyższonej temperaturze pomiędzy 90 i 630°C prowadzi do gwałtownego spadku modułu Younga dla temperatury wyżarzania powyżej 210°C. Po wyżarzaniu w 410°C,  $E$  osiąga minimalną wartość, która jest o 35% niższa niż wartość  $E$  w próbkach CGFA (całkowita zmiana  $E$  wynosi około 47% wartości początkowej). Dalsze wyżarzanie w wyższych temperaturach prowadzi do zwiększenia modułu Younga. Pokazano, że to niezwykle zachowanie modułu Younga jest spowodowane tworzeniem osiowej tekstury  $\langle 111 \rangle$  w próbkach poddanych SPD, która następnie zastępowana jest teksturą  $\langle 001 \rangle$  podczas obróbki cieplnej po SPD.

## 1. Introduction

Severe plastic deformation (SPD) is the most accessible way of obtaining bulk ultrafine-grained (UFG) metals and alloys. However, SPD-processed metals and alloys have non-equilibrium defect structures that cause time and thermal instability of functional and operational characteristics of these materials. That is why, a study of SPD-induced microstructures, and their stability is an important problem of material science both from fundamental and engineering points of view.

Young's modulus  $E$  is a structure-sensitive parameter giving integral information on volume properties of the materials. Till now, main attention was concentrated on studying the behavior of dynamic components of Young's modulus caused by relaxation processes in various subsystems of materials. Beyond of the attention remains the problem of influence of textures that may develop in the UFG metals at different stages of their preparation and post-SPD treatment.

In the present work, an influence of annealing on the dynamic Young's modulus of UFG copper wires prepared by the repeated hydrostatic extrusion and drawing is investigated. Non-trivial behavior of Young's modulus is revealed in comparison with the results obtained on the processed by equal-channel angular pressing (ECAP) UFG copper [1-4]. It is established that the unusual behavior of the elastic properties is due to the formation of the  $\langle 111 \rangle$  axial texture in the samples subjected to SPD and its subsequent transformation into the  $\langle 001 \rangle$  axial texture during annealing at elevated temperatures.

## 2. Experimental

### 2.1. Sample preparation

Wires from the UFG Fire Refined Tough Pitch (FRTP) copper were obtained using the combined SPD treatment that involved repeated cold hydrostatic extrusion (HE) and drawing

\* B. VERKIN INSTITUTE FOR LOW TEMPERATURE PHYSICS AND ENGINEERING, 61103 KHARKOV, UKRAINE

\*\* A. GALKIN DONETSK PHYSICO-TECHNICAL INSTITUTE, 83114 DONETSK, UKRAINE

\*\*\* S. KUZNETS KHARKOV NATIONAL UNIVERSITY OF ECONOMICS, 61166 KHARKOV, UKRAINE

<sup>#</sup> Corresponding author: palval@ilt.kharkov.ua

(D). Total reduction in the initial billet cross-section was 99.89 % that corresponds to the cumulative deformation  $e = 6.77$ . The mean grain size was  $d \sim 200 - 300$  nm.

## 2.2. Acoustic measurements

Measurements of Young's modulus were carried out using the two-component composite oscillator technique. Longitudinal standing waves were excited in the samples of 25 mm in length and 2 mm in diameter at frequencies  $f \approx 70$  kHz by means of a piezoelectric transducer. The ultrasound wave vector coincided with the direction of hydrostatic extrusion and drawing. Temperature dependences of the dynamic Young's modulus  $E(T)$  were measured in the temperature interval 5 – 310 K at constant ultrasonic strain amplitude  $\varepsilon_0 \sim 1 \cdot 10^{-7}$  in the amplitude independent range. The heating rate was about 1 K/min.

## 2.3. Post-SPD heat treatment

At first, the measurements were carried out on the as-prepared samples. Then they were repeated after several 30 min isothermal anneals in vacuum at elevated annealing temperatures  $T_{\text{ann}}$  in the interval from 90 to 630°C with the step from 10 to 20°C. As it was done in [4], the interval of  $T_{\text{ann}}$  was firstly chosen in such a way that the expected temperature of the primary recrystallization  $T_R \approx 135^\circ\text{C}$  lied in the middle of the interval. However, the behavior of Young's modulus when annealing samples prepared by hydrostatic extrusion and drawing was cardinally different from that in the ECAP-processed copper. That is why the interval of  $T_{\text{ann}}$  was extended towards appreciably higher temperatures.

## 3. Results

Temperature dependences of Young's modulus are shown in Fig. 1 (for clarity, some dependences are not there shown). For comparison, dependences  $E(T)$  obtained on the ECAP-processed copper (curve ECAP-4) [4] and coarse-grained fully annealed Cu (curve CGFA) [5] are cited in Fig. 1 as well. Young's modulus of the wires obtained by hydrostatic extrusion and drawing appeared to be more than 20 % **higher** than corresponding values of  $E$  in the CGFA samples. Isothermal annealing at elevated temperatures led to the non-monotonic changes in Young's modulus. Up to  $T_{\text{ann}} = 150^\circ\text{C}$ , Young's modulus slightly increased. During further increasing of the  $T_{\text{ann}}$ , Young's modulus values began to decrease, at first, rather slowly. Then rate of Young's modulus drop  $dE/dT_{\text{ann}}$  increased sharply and finally the dependence  $E(T)$  appeared to be essentially **below** the curve obtained on CGFA samples. The total reduction of Young's modulus from its maximum down to minimum values amounts to 47 % (see Fig. 2).

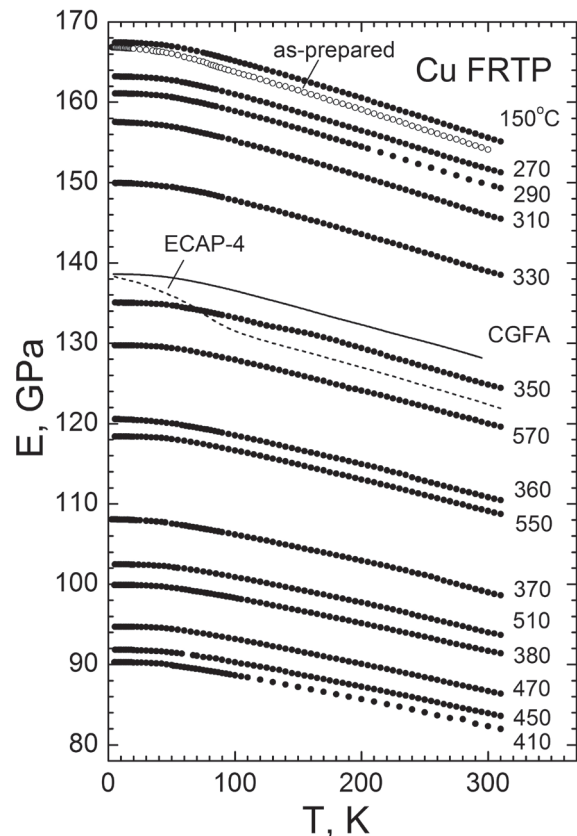


Fig. 1. Variation of Young's modulus in the UFG copper wire: (○) – as-prepared; (●) – after isothermal annealing at temperatures indicated close to the curves; ECAP-4 –  $E(T)$  in the UFG copper after four ECAP runs [4]; CGFA –  $E(T)$  in the coarse-grained fully annealed texture-free copper [5].

## 4. Discussion

### 4.1. Abnormal changes in Young's modulus value

Usually, intensive plastic deformation leads to essential reduction in Young's modulus of UFG metals [1-4,6]. In experiments on the ECAP-processed copper [1-4], it was shown that Young's modulus decreases, mainly, due to a considerable increase in dislocation density. The dislocation nature of the dynamic Young's modulus reduction was proved when studying the Bordoni acoustic relaxation in the ECAP-processed copper [3,4]. The maximum reduction of Young's modulus was observed at  $T > T_B$  ( $T_B \approx 89$  K). In the low-temperature limit ( $T \rightarrow 5$  K), the relaxation process (thermally activated kink pair formation on dislocations) is "frozen" and the modulus defect diminishes as it can be seen in Fig. 1, curve ECAP-4. Subsequent annealing of the ECAP-4 samples at elevated temperatures led to a significant reduction of the dislocation density and to increase of the effective Young's modulus. The dependence  $E(T)$  approached that in the CGFA samples and they almost coincided after annealing at  $T_{\text{ann}} > 150^\circ\text{C}$ .

Entirely different behavior was observed in the present work. After SPD-processing, unexpectedly high values of Young's modulus were registered and their huge reduction at high-temperature annealing was revealed (Fig. 2).

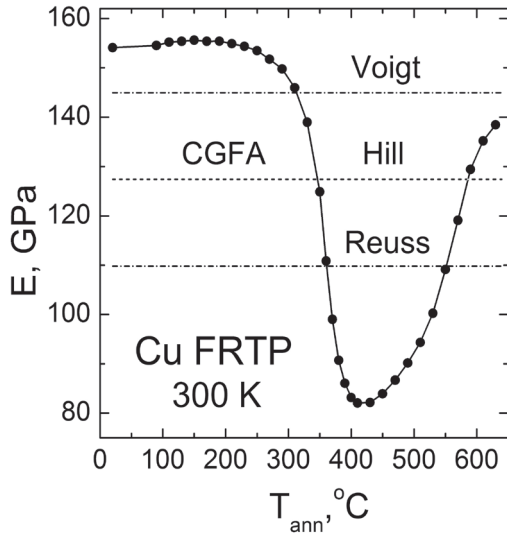


Fig. 2. Effect of annealing temperature on Young's modulus at 300 K. Dashed line indicates the value of  $E$  in the CGFA copper [4,5] and dash-dotted lines show the Voigt's (upper) and Reuss' (lower) averaged values.

To explain these experimental results, let us consider, firstly, the problem of possible limits of Young's modulus variations in the crystalline copper. The orientation dependence of Young's modulus of the crystals with cubic symmetry can be expressed as [7]:

$$E^{<hkl>} = \left[ \frac{(C_{11} + C_{12})}{(C_{11} + 2C_{12})(C_{11} - C_{12})} + r \left( \frac{1}{C_{44}} - \frac{2}{C_{11} - C_{12}} \right) \right]^{-1}, \quad (1)$$

where  $C_{11}$ ,  $C_{12}$  and  $C_{44}$  are the components of the elastic stiffness tensor,  $r = l_{11}^2 l_{12}^2 + l_{11}^2 l_{13}^2 + l_{12}^2 l_{13}^2$ , where  $l_{ij}$  denotes the direction cosines. Young's modulus has extrema for the crystallographic directions  $\langle 001 \rangle$  and  $\langle 111 \rangle$ .

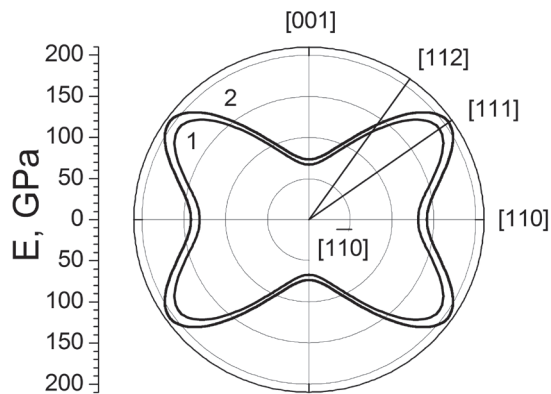


Fig. 3. Sections of the copper Young's modulus characteristic surfaces by the  $(1 \bar{1} 0)$  plane at 300 K (line 1) and 5 K (line 2)

The sections of the characteristic Young's modulus surfaces for copper by the  $(1 \bar{1} 0)$  plane are presented in Fig. 3. The plot shows that Young's modulus has the maximum in the direction  $\langle 111 \rangle$  and the minimum in the direction  $\langle 001 \rangle$ :  $E^{\langle 111 \rangle} = 205.0$  and  $191.4$  GPa,  $E^{\langle 001 \rangle} = 73.2$  and  $67.0$  GPa at 5 and 300 K, respectively. Thus, the values of  $E$  obtained in our experiment appear to be within the possible limits of Young's modulus in copper single crystal.

## 4.2. Young's modulus of polycrystals

If a polycrystalline body consists of a large number of randomly oriented grains, it may be considered as a quasi-isotropic medium, which elastic properties can be characterized by the effective elastic coefficients. Voigt and Reuss suggested two averages of elastic properties of the quasi-isotropic polycrystals that determine the upper ( $E_V$ ) and lower ( $E_R$ ) boundaries for the elastic moduli of quasi-isotropic polycrystals. For the cubic polycrystals, they may be expressed through the single crystal elastic constants as

$$E_V = \frac{(C_{11} + 2C_{12})(C_{11} - C_{12} + 3C_{44})}{2C_{11} + 3C_{12} + C_{44}}, \quad (2)$$

$$E_R = \frac{5C_{44}(C_{11} + 2C_{12})(C_{11} - C_{12})}{C_{11}(C_{11} + 3C_{44}) + C_{12}(C_{11} - 2C_{12} + C_{44})}. \quad (3)$$

For more realistic estimation of  $E$ , Hill used the arithmetic or geometric mean of  $E_V$  and  $E_R$ :

$$E_{VRH}^A = \frac{E_V + E_R}{2}; \quad E_{VRH}^G = \sqrt{E_V E_R}. \quad (4a,4b)$$

The measured after SPD values of  $E$  are higher than the upper boundary  $E_V$ . In the samples annealed at  $T_{ann} \geq 370$  °C, Young's modulus falls to the values that lie well below  $E_R$  (see Fig. 2; the Hill arithmetic averaging almost coincides with the CGFA curve). It means that SPD-processing leads to a formation in the samples of a structure with pronounced anisotropy of elastic properties. Annealing of the samples does not lead to a formation of a quasi-isotropic state but, per contra, promotes some transition into another anisotropic state with very low values of Young's modulus.

Anisotropy of the elastic properties of the polycrystalline samples may be caused by formation of the pronounced  $\langle 111 \rangle$  axial crystallographic texture as a result of heavy plastic deformation. Annealing at elevated temperatures leads to the transformation of the  $\langle 111 \rangle$  texture into the  $\langle 001 \rangle$  axial texture that becomes prevailing for annealing temperatures above 360 °C up to 410 °C. At higher annealing temperatures, some intermediate crystallographic textures begin to dominate.

These assumptions agree rather well with the results of a texture analysis of the microcrystalline copper wires obtained by drawing and then annealed [8]. According to [8], the central part of the wire may be regarded as a composite material with the fibers having  $\langle 001 \rangle$  and  $\langle 111 \rangle$  orientations along the wire axis. In the peripheral zone, the  $\langle 112 \rangle$  orientation

is dominating. During annealing, volume fractions of  $\langle 111 \rangle$  and  $\langle 001 \rangle$  orientations in the central zone radically changes and after annealing at  $T_{\text{ann}} > 350^\circ\text{C}$  the  $\langle 001 \rangle$  axial texture becomes dominating. Estimations made in the fiber composite approximation show that after the deformation the volume fractions of  $\langle 111 \rangle$  and  $\langle 001 \rangle$  textures are 62 % and 18 %, respectively. After annealing at  $410^\circ\text{C}$ , they change to 3.2 % and 76.8 %.

### 5. Summary

In contrast to the ECAP processed copper, Young's modulus  $E$  of the samples prepared by repeated hydrostatic extrusion and drawing **increases** up to 20 % as compared to that in the coarse-grained fully annealed (CGFA) copper.

Isothermal annealing at temperatures up to  $150^\circ\text{C}$  leads to an additional slight (less than 1 %) growth of Young's modulus. This increase of  $E$  is caused mainly by an essential decrease of the dislocation density in the samples. After annealing at higher temperatures, Young's modulus falls down to the values 35 % smaller than those in the CGFA samples.

Comparison with the texture analysis made for the microcrystalline copper wires shows that the very high values of  $E$  in the deformed samples are due to the formation of the  $\langle 111 \rangle$  crystallographic axial texture having the highest Young's modulus in copper. Significant reduction of  $E$  when annealing the samples is caused by the replacement of the  $\langle 111 \rangle$  axial texture by the  $\langle 001 \rangle$  one.

### REFERENCES

- [1] N. Kobelev, E. Kolyvanov, Y. Estrin, Temperature dependence of sound attenuation and shear modulus of ultra fine grained copper produced by equal channel angular pressing, *Acta Materialia*, **56**, 1473-1481 (2008).
- [2] E.N. Vatazhuk, P.P. Pal-Val, L.N. Pal-Val, V.D. Natsik, M.A. Tikhonovsky, A.A. Kupriyanov, Low-temperature relaxation processes in a Cu-Nb nanostructured fiber composite, *Low Temp. Phys.* **35**, 417-423 (2009).
- [3] I.S. Golovin, P.P. Pal-Val, L.N. Pal-Val, E.N. Vatazhuk, Y. Estrin, The effect of annealing on the internal friction in ECAP-modified ultrafine grained copper, *Solid State Phenomena* **184**, 289-294 (2012).
- [4] P.P. Pal-Val, L.N. Pal-Val, Low-temperature internal friction and nanostructured metal stability, *Metal Science and Heat Treatment* **54**, 234-238 (2012).
- [5] H.M. Ledbetter, Elastic constants of polycrystalline copper at low temperatures. Relationship to single-crystal elastic constants, *Phys. Stat. Sol. (a)* **66**, 477-484 (1981).
- [6] Y.A. Burenkov, S.P. Nikanorov, B.I. Smirnov, V.I. Kopylov, Recovery of Young's modulus upon annealing of nanostructured niobium produced through severe plastic deformation. *Phys Solid State* **45**, 2119-2123 (2003).
- [7] L.D. Landau, E.M. Lifshitz, *Theory of Elasticity*, Pergamon Press, Oxford, 1970, p. 43.
- [8] S.L. Demakov, Y.N. Loginov, A.G. Illarionov, M.A. Ivanova, M.S. Karabanalov, Effect of annealing temperature on the texture of copper wire. *Phys. Metals Metallogr.* **113**, 681-686 (2012).